Suppression of magneto-optical transport in tilted Weyl semimetals by orbital magnetic moment

Yang Gao,[1,*] Zhi-Qiang Zhang,[2,3] Hua Jiang,[2,3] and Kai-He Ding[4,†]

[1]*College of Computer Science and Engineering, Anhui University of Science and Technology, Huainan 232001, China*

[2]*School of Physical Science and Technology, Soochow University, Suzhou 215006, China*

[3]*Institute for Advanced Study, Soochow University, Suzhou 215006, China*

[4]*Department of Physics and Electronic Science, Changsha University of Science and Technology, Changsha 410076, China*

(Received 30 December 2021; accepted 11 April 2022; published 21 April 2022)

By incorporating the orbital magnetic moment, we investigate the magneto-optical transport of Weyl semimetals within a semiclassical approximation. In the linear or nonlinear response regime, an analytic expression for the magnetoconductivity is obtained, where a new term due to the orbital magnetic moment is added, and leads to a partial cancellation for the total magnetoconductivities. This suppressed feature is further manifested by analyzing the linear and quadratic contribution in the magnetic field to magnetoconductivities. This result may be used to explain the deviation between the recent theory and experiment.

DOI: 10.1103/PhysRevB.105.165307

I. INTRODUCTION

Weyl semimetals are a newly discovered class of topological materials with pairs of conduction and valence bands touching at the discrete points in the Brillouin zone (called Weyl points) [1–8], around which the dispersion relation is linear. This special band structure gives rise to a nontrivial topological property, which can be identified by the Berry curvature that is usually considered as an effective magnetic field in the momentum-space with a monopole located at the Weyl node. According to the Nielsen-Ninomiya theorem [9,10], the Weyl nodes always appear in pairs, and form a source and sink of this effective field, respectively, which leads to a number of the unusual phenomena, such as high mobility phenomena [11,12], the existence of Fermi arcs [4–8], the chiral anomaly [13–16], and the anomalous Hall effect [17,18], etc.

The discovery of Weyl semimetals triggers a search for a variety of novel quantum phenomenon. As an important aspect, the magneto-electronic transport properties have been quickly a focus of interest. A series of phenomena related to the chiral anomaly is revealed successively. For example, the negative magnetoresistance has been experimentally observed in Weyl semimetal materials [19–23]. The planar Hall effect is predicted theoretically in Weyl semimetals, in which a nonzero Hall conductivity has emerged in the plane of the electric and magnetic fields [24–29]. Additionally, the anomalous Nernst effect has been studied both theoretically and experimentally [30–38].

Recently, much attention has been paid to the research of the nonlinear magneto-optical responses in the Weyl semimetal materials. In the absence of external magnetic fields, the second-order optical response in the Weyl semimetals involves injection, shift, and anomalous current. Interestingly, all these quantities relate to the topological effect of Weyl semimetals, and require breaking inversion symmetry. The injection current is proportional to the Berry curvature and the difference of the velocities of electrons between the conduction band and valence band in Weyl semimetals [39–44]. The shift current stems from a combined effect of the linear photoabsorption and the shift vector (defined by Berry connections) [41,45,46], and has been confirmed by observing a strong second harmonic signal in TaAs [47]. The nonlinear anomalous current (nonlinear Hall effect) arises from the Berry curvature dipole [48–56], and has been observed in the materials WTe_2 and Cd_3As_2 [57–59]. Under the weak magnetic field, the optical activity and the chiral anomaly will contribute to the second-order nonlinear optical response in the Weyl semimetal [60–63]. Whereas in a strong magnetic field, the third-order responses have an extremely high optical susceptibility originating from the linear energy dispersion near the Weyl nodes [64,65].

It is known that the "self-rotation" of the Bloch wave packet will induce an orbital magnetic moment [66], and modify the energy of the electron under the external magnetic field, which will change the magneto-optical responses of tilted Weyl semimetals, an issue which is addressed here.

In this paper, we study the linear and nonlinear magneto-optical responses for tilted Weyl semimetals, where an orbital magnetic moment is introduced. We derive an analytic expression for the magnetoconductivity by means of the Boltzmann equation method. It is found that the orbital magnetic moment induces a new magnetoconductivity term, which gives rise to a partial cancellation for the total magnetoconductivity. This suppressed feature is further manifested by analyzing the linear (*B*-linear) and quadratic (quadratic-*B*) contribution in the magnetic field to magnetoconductivities. We also show that no matter in the linear or nonlinear response regime, the *B*-linear (quadratic-*B*) magnetoconductivity exhibits a behavior that is dependent (independent) of the chirality of the Weyl node.

*gao_yang_good@126.com

†dingkh@csust.edu.cn

The paper is organized as follows: In Sec. II, we begin with the model of a 3D Weyl semimetal with a tilt in the z direction, and then the semiclassical equations of motion for the dynamics of the electron wave packet in the electric and magnetic fields are presented. In Sec. III, the B-linear and quadratic-B magnetoconductivities including the orbital magnetic moment are obtained in the linear response regime, and analyzed in detail. In Sec. IV, we study second harmonic generation, and give the second harmonic conductivity formula as well as the further analysis for this result. We end with conclusions in Sec. V.

II. MODEL AND METHOD

A. Weyl semimetals and the semiclassical equations of motion

We consider the effective low-energy continuum Hamiltonian for a 3D Weyl semimetal with a tilt in the z direction, which takes the form [67–70]

$$H_0(\boldsymbol{k}) = s\hbar v_F \boldsymbol{k}\cdot\boldsymbol{\sigma} + \hbar v_F t_s k_z \sigma_0, \tag{1}$$

where $s = \pm$ is the chirality of the valley, v_F is the Fermi velocity, $\boldsymbol{k}$ is the momentum, σ_0 is a 2×2 identity matrix and $\boldsymbol{\sigma}$ are the Pauli matrices. We use t_s $[t_s \in [0,1)]$ to describe the tilt of Weyl cones. The case with parameter $t_+ = -t_- = t$ respects tilt inversion symmetry and the case with parameter $t_+ = t_- = t$ breaks tilt inversion symmetry [70]. The eigenvalue of the Hamiltonian (1) is $\varepsilon^s_{\boldsymbol{k}} = \hbar v_F(t_s k_z + nk)$ with $n = \pm 1$ labeling the conduction and valence bands, respectively.

The semiclassical equations of motion for the electron wave packet at the location $\boldsymbol{r}$ and the wave vector $\boldsymbol{k}$ in a given band are [66,71]

$$\dot{\boldsymbol{r}} = \frac{1}{\hbar}\nabla_k \tilde{\varepsilon}^s_{\boldsymbol{k}} - \dot{\boldsymbol{k}}\times\boldsymbol{\Omega}^s_{\boldsymbol{k}}, \tag{2}$$

$$\hbar\dot{\boldsymbol{k}} = -e\boldsymbol{E} - e\dot{\boldsymbol{r}}\times\boldsymbol{B}, \tag{3}$$

where $-e$ is the electron charge, $\boldsymbol{E}$ and $\boldsymbol{B}$ are external electric and magnetic fields, respectively. $\boldsymbol{\Omega}^s_{\boldsymbol{k}}$ is the Berry curvature, and $\tilde{\varepsilon}^s_{\boldsymbol{k}} = \varepsilon^s_{\boldsymbol{k}} - \boldsymbol{m}^s_{\boldsymbol{k}}\cdot\boldsymbol{B}$ with the orbital magnetic moment $\boldsymbol{m}^s_{\boldsymbol{k}}$ induced by the semiclassical "self-rotation" of the Bloch wave packet [66]:

$$\boldsymbol{\Omega}^s_{\boldsymbol{k}} = -\mathrm{Im}\big[\langle\nabla_k u^s_{\boldsymbol{k}}| \times |\nabla_k u^s_{\boldsymbol{k}}\rangle\big], \tag{4}$$

$$\boldsymbol{m}^s_{\boldsymbol{k}} = -\frac{e}{2\hbar}\mathrm{Im}\big[\langle\nabla_k u^s_{\boldsymbol{k}}| \times \big(H_0(\boldsymbol{k}) - \varepsilon^s_{\boldsymbol{k}}\big)|\nabla_k u^s_{\boldsymbol{k}}\rangle\big], \tag{5}$$

where $|u^s_{\boldsymbol{k}}\rangle$ satisfies the equation $H_0(\boldsymbol{k})|u^s_{\boldsymbol{k}}\rangle = \varepsilon^s_{\boldsymbol{k}}|u^s_{\boldsymbol{k}}\rangle$. By solving these coupled equations (2) and (3), one obtains

$$\dot{\boldsymbol{r}} = \frac{1}{\hbar D}\Big[\nabla_k\tilde{\varepsilon}^s_{\boldsymbol{k}} + e\boldsymbol{E}\times\boldsymbol{\Omega}^s_{\boldsymbol{k}} + \frac{e}{\hbar}\big(\nabla_k\tilde{\varepsilon}^s_{\boldsymbol{k}}\cdot\boldsymbol{\Omega}^s_{\boldsymbol{k}}\big)\boldsymbol{B}\Big], \tag{6}$$

$$\dot{\boldsymbol{k}} = \frac{1}{\hbar D}\Big[-e\boldsymbol{E} - \frac{e}{\hbar}\nabla_k\tilde{\varepsilon}^s_{\boldsymbol{k}}\times\boldsymbol{B} - \frac{e^2}{\hbar}(\boldsymbol{E}\cdot\boldsymbol{B})\boldsymbol{\Omega}^s_{\boldsymbol{k}}\Big], \tag{7}$$

where the factor $D = 1 + e/\hbar(\boldsymbol{\Omega}^s_{\boldsymbol{k}}\cdot\boldsymbol{B})$ modifies the phase space volume [72].

B. Boltzmann equation under optical field

We suppose that a static magnetic field $\boldsymbol{B}$ and a light field $\boldsymbol{E}(t) = \boldsymbol{E}(\omega)e^{-i\omega t}$ are simultaneously applied to Weyl semimetals. The distribution function of electrons $\tilde{f}^s$ obeys the semiclassical Boltzmann kinetic equation

$$\frac{\partial\tilde{f}^s}{\partial t} + \dot{\boldsymbol{k}}\frac{\partial\tilde{f}^s}{\partial\boldsymbol{k}} = -\frac{\tilde{f}^s - \tilde{f}^s_0}{\tau}, \tag{8}$$

where τ is the relaxation time originating from the scattering of electrons by phonons, impurities, electrons, and other lattice imperfections [73]. $\tilde{f}^s_0(\tilde{\varepsilon}^s_{\boldsymbol{k}})$ is the Fermi-Dirac distribution function for the energy $\tilde{\varepsilon}^s_{\boldsymbol{k}}$, and at the low magnetic field expanded as [71,74,75]

$$\begin{aligned}\tilde{f}^s_0 &= f^s_0\big(\varepsilon^s_{\boldsymbol{k}} - \boldsymbol{m}^s_{\boldsymbol{k}}\cdot\boldsymbol{B}\big)\\ &\simeq f^s_0\big(\varepsilon^s_{\boldsymbol{k}}\big) - \boldsymbol{m}^s_{\boldsymbol{k}}\cdot\boldsymbol{B}\frac{\partial f^s_0\big(\varepsilon^s_{\boldsymbol{k}}\big)}{\partial\varepsilon^s_{\boldsymbol{k}}},\end{aligned} \tag{9}$$

where $f^s_0 = f^s_0(\varepsilon^s_{\boldsymbol{k}}) = 1/[e^{(\varepsilon^s_{\boldsymbol{k}}-\mu)/k_BT} + 1]$ with k_B the Boltzmann constant, T the temperature, and μ the chemical potential.

Equation (8) can be solved by expanding the distribution function in a power series in the electric field as follows:

$$\tilde{f}^s = \tilde{f}^s_0 + \tilde{f}^s_1 e^{-i\omega t} + \tilde{f}^s_2 e^{-2i\omega t} + \cdots, \tag{10}$$

where $\tilde{f}^s_1$ and $\tilde{f}^s_2$ are the first- and second-order terms for $\boldsymbol{E}$, respectively. The electric current density can be calculated by

$$\boldsymbol{j} = -e\int[d\boldsymbol{k}]D\dot{\boldsymbol{r}}\tilde{f}^s, \tag{11}$$

where $[d\boldsymbol{k}] = d\boldsymbol{k}/(2\pi)^3$. Equations (8) and (11) establish a basis for studying transport properties under the combined influence of the external magnetic and electric fields.

III. LINEAR RESPONSE OF WEYL SEMIMETALS

Firstly, we focus on linear responses driven by monochromatic light at the frequency ω. Substituting Eq. (7) into Eq. (8) and retaining terms up to first order in $\boldsymbol{E}$, we obtain

$$\frac{1}{\hbar D}\Big[-e\boldsymbol{E} - \frac{e^2}{\hbar}(\boldsymbol{E}\cdot\boldsymbol{B})\boldsymbol{\Omega}^s_{\boldsymbol{k}}\Big]\cdot\frac{\partial\tilde{f}^s_0}{\partial\boldsymbol{k}} - i\omega\tilde{f}^s_1 = -\frac{\tilde{f}^s_1}{\tau}. \tag{12}$$

It is noted that the $\tilde{\boldsymbol{v}}^s_{\boldsymbol{k}}\times\boldsymbol{B}$ term vanishes in the square brackets of Eq. (12) since it is perpendicular to $(1/\hbar)\partial_{\boldsymbol{k}}\tilde{f}^s_0$ [61]. However, it exists for the first-order correction $\tilde{f}^s_1$, and will give rise to the ordinary Hall current, which depends on $\omega_c\tau$ (here $\omega_c = eBv_F^2/\mu$ is the cyclotron frequency). For the case of only intranode scattering, the cyclotron motion can be neglected at $\mu\tau/\hbar \ll 1$ [25–27]. Furthermore, from Eq. (12), it can be observed that the term $\tilde{\boldsymbol{v}}^s_{\boldsymbol{k}}\times\boldsymbol{B}$ does not couple to the other ones related to the Berry curvature. Thus for the simplicity, we ignore the ordinary Hall term. A further calculation for Eq. (12) gives

$$\tilde{f}^s_1 = \frac{\tau}{1 - i\omega\tau}\frac{1}{\hbar D}\Big[e\boldsymbol{E} + \frac{e^2}{\hbar}(\boldsymbol{E}\cdot\boldsymbol{B})\boldsymbol{\Omega}^s_{\boldsymbol{k}}\Big]\cdot\frac{\partial\tilde{f}^s_0}{\partial\boldsymbol{k}}. \tag{13}$$

At the low magnetic field, we expand Eq. (13) up to the second order in $\boldsymbol{B}$, and find

$$\tilde{f}_1^s = \frac{\tau}{1-i\omega\tau}\Big[e\boldsymbol{E}\cdot\boldsymbol{v}_{\boldsymbol{k}}^s\frac{\partial f_0^s}{\partial\varepsilon_{\boldsymbol{k}}^s} - \frac{e^2}{\hbar}(\boldsymbol{B}\cdot\boldsymbol{\Omega}_{\boldsymbol{k}}^s)(\boldsymbol{E}\cdot\boldsymbol{v}_{\boldsymbol{k}}^s)\frac{\partial f_0^s}{\partial\varepsilon_{\boldsymbol{k}}^s} + \frac{e^2}{\hbar}(\boldsymbol{E}\cdot\boldsymbol{B})(\boldsymbol{\Omega}_{\boldsymbol{k}}^s\cdot\boldsymbol{v}_{\boldsymbol{k}}^s)\frac{\partial f_0^s}{\partial\varepsilon_{\boldsymbol{k}}^s} - \frac{e}{\hbar}\boldsymbol{E}\cdot\frac{\partial}{\partial\boldsymbol{k}}\Big(\boldsymbol{m}_{\boldsymbol{k}}^s\cdot\boldsymbol{B}\frac{\partial f_0^s}{\partial\varepsilon_{\boldsymbol{k}}^s}\Big)$$
$$-\frac{e^3}{\hbar^2}(\boldsymbol{B}\cdot\boldsymbol{\Omega}_{\boldsymbol{k}}^s)(\boldsymbol{E}\cdot\boldsymbol{B})(\boldsymbol{\Omega}_{\boldsymbol{k}}^s\cdot\boldsymbol{v}_{\boldsymbol{k}}^s)\frac{\partial f_0^s}{\partial\varepsilon_{\boldsymbol{k}}^s} + \frac{e^3}{\hbar^2}(\boldsymbol{B}\cdot\boldsymbol{\Omega}_{\boldsymbol{k}}^s)^2(\boldsymbol{E}\cdot\boldsymbol{v}_{\boldsymbol{k}}^s)\frac{\partial f_0^s}{\partial\varepsilon_{\boldsymbol{k}}^s} + \frac{e^2}{\hbar^2}(\boldsymbol{B}\cdot\boldsymbol{\Omega}_{\boldsymbol{k}}^s)\boldsymbol{E}\cdot\frac{\partial}{\partial\boldsymbol{k}}\Big(\boldsymbol{m}_{\boldsymbol{k}}^s\cdot\boldsymbol{B}\frac{\partial f_0^s}{\partial\varepsilon_{\boldsymbol{k}}^s}\Big)$$
$$-\frac{e^2}{\hbar^2}(\boldsymbol{E}\cdot\boldsymbol{B})\boldsymbol{\Omega}_{\boldsymbol{k}}^s\cdot\frac{\partial}{\partial\boldsymbol{k}}\Big(\boldsymbol{m}_{\boldsymbol{k}}^s\cdot\boldsymbol{B}\frac{\partial f_0^s}{\partial\varepsilon_{\boldsymbol{k}}^s}\Big)\Big]. \tag{14}$$

From Eqs. (6) and (14), the current density at the frequency ω is given by

$$\boldsymbol{j}_1 = -e\int[d\boldsymbol{k}]\Big[\tilde{\boldsymbol{v}}_{\boldsymbol{k}}^s + \frac{e}{\hbar}(\tilde{\boldsymbol{v}}_{\boldsymbol{k}}^s\cdot\boldsymbol{\Omega}_{\boldsymbol{k}}^s)\boldsymbol{B}\Big]\tilde{f}_1^s$$
$$-\frac{e^2}{\hbar}\int[d\boldsymbol{k}]\boldsymbol{E}\times\boldsymbol{\Omega}_{\boldsymbol{k}}^s\tilde{f}_0^s, \tag{15}$$

whose component is simply expressed as

$$\boldsymbol{j}_a(\omega) = \sigma_{ab}(\omega)E_b(\omega), \tag{16}$$

where $\sigma_{ab}(\omega)$ is the frequency-dependent conductivity. It is known that the single contribution from the group velocity $\tilde{\boldsymbol{v}}_{\boldsymbol{k}}^s$ or the Berry curvature $\boldsymbol{\Omega}_{\boldsymbol{k}}^s$ form the conventional longitudinal or Hall conductivities. In the presence of the magnetic field, the conductivity $\sigma(\omega)$ consists of the coupling terms between the group velocity $\tilde{\boldsymbol{v}}_{\boldsymbol{k}}^s$ and the Berry curvature $\boldsymbol{\Omega}_{\boldsymbol{k}}^s$ besides the conventional ingredients [see Eq. (15)]. Their combined contributions are triggered by the external magnetic field, and play a crucial role in the electron transport (see below).

A. The conductivity $\sigma_{ab}^{(0)}$ in absence of magnetic field

Substituting Eq. (14) into the first term of Eq. (15) and keeping $\boldsymbol{B} = 0$, the conductivity tensor linking the Cartesian components is given by

$$\sigma_{ab}^{(0)}(\omega) = \frac{e^2\tau}{1-i\omega\tau}\int[d\boldsymbol{k}]v_a^s v_b^s\Big(-\frac{\partial f_0^s}{\partial\varepsilon_{\boldsymbol{k}}^s}\Big). \tag{17}$$

At $T = 0$, owing to $-\partial f_0^s/\partial\varepsilon_{\boldsymbol{k}} = \delta(\varepsilon_{\boldsymbol{k}}^s - \mu)$, we arrive at

$$\sigma_{zz}^{(0)}(\omega) = \frac{\sigma_D}{t_s^3}\Big[-3t_s - \frac{3}{2}\ln\frac{1-t_s}{1+t_s}\Big], \tag{18}$$

$$\sigma_{xx}^{(0)}(\omega) = \frac{\sigma_D}{t_s^3}\Big[-\frac{3t_s}{2(t_s^2-1)} + \frac{3}{4}\ln\frac{1-t_s}{1+t_s}\Big], \tag{19}$$

and $\sigma_{xx}^{(0)}(\omega) = \sigma_{yy}^{(0)}(\omega)$, where the Drude frequency dependent complex conductivity is

$$\sigma_D = \frac{e^2\tau\mu^2}{(1-i\omega\tau)6\pi^2\hbar^3 v_F}. \tag{20}$$

Equations (18) and (19) are in consistent with the results of Refs. [27,76,77]. Figure 1(a) shows a comparison on the tilt t_+ dependence of $\sigma_{xx}^{(0)}(\omega)$ and $\sigma_{zz}^{(0)}(\omega)$. For $t_s \to 0$, $\sigma_{xx}^{(0)}(\omega) = \sigma_{zz}^{(0)}(\omega) = \sigma_D$. When t_s is taken into account, the system becomes anisotropic [see Hamiltonian (1)], and so there appears a difference between the conductivities $\sigma_{xx}^{(0)}(\omega)$ and $\sigma_{zz}^{(0)}(\omega)$, which is greatly enhanced with increasing t_s. From Eqs. (18) and (19), one also finds that $\sigma_{aa}^{(0)}(\omega)$ is even with respect to the tilt t_s, reflecting the chirality symmetry of the system. Thus, the total conductivity is twice the contribution from a single Weyl node. In addition, similar to the usual metals, the frequency dependence of the conductivity $\sigma_{aa}^{(0)}(\omega)(a = x, z)$ exhibits a Drude-type behavior, as shown in Fig. 1(b). In the Weyl semimetals, we have the relaxation time $\tau \sim 10^{-13}$ s, and the Fermi velocity $v_F \sim 10^5$ m/s [25–27]. When the Fermi energy is taken as $\mu = 1$ meV, the conductivity is estimated as $\sigma_{xx}^{(0)} \simeq 2.4\ \Omega^{-1}\,\mathrm{m}^{-1}$ at $\omega \to 0$.

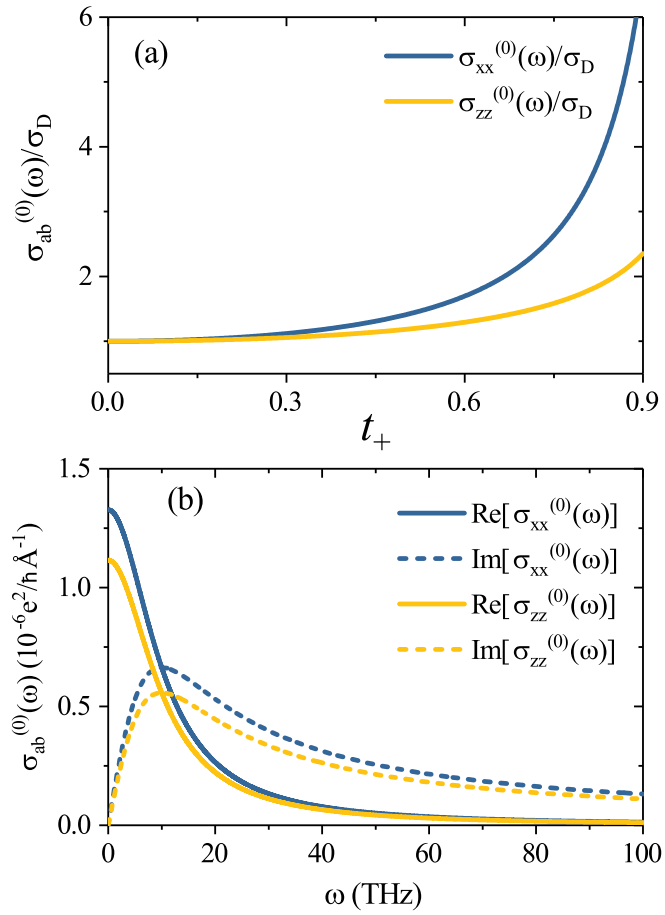

FIG. 1. (a) The dependence of the conductivity on the tilt t_+[see Eqs. (18) and (19)]. (b) The frequency dependence of optical conductivity at $t_+ = 0.5$. The other parameters are taken as $v_F = 4.13 \times 10^5$ m/s, $\mu = 1$ meV and $\tau = 10^{-13}$ s.

B. *B*-linear contribution to the conductivity $\sigma_{ab}^{(B)}$

For a weak magnetic field, substituting Eq. (14) into the first term of Eq. (15), we only keep the linear order terms in $\boldsymbol{B}$. The magnetoconductivity is then given by

$$\sigma_{ab}^{(B)}(\omega) = \sigma_{ab}^{(B,\Omega)}(\omega) + \sigma_{ab}^{(B,m)}(\omega), \tag{21}$$

where

$$\sigma_{ab}^{(B,\Omega)}(\omega) = \frac{e^3\tau}{\hbar(1-i\omega\tau)} \int [d\boldsymbol{k}]\left[\left(v_a^s B_b + v_b^s B_a\right)\left(\boldsymbol{v}_{\boldsymbol{k}}^s \cdot \boldsymbol{\Omega}_{\boldsymbol{k}}^s\right) - v_a^s v_b^s \left(\boldsymbol{B}\cdot\boldsymbol{\Omega}_{\boldsymbol{k}}^s\right)\right]\left(-\frac{\partial f_0^s}{\partial \varepsilon_{\boldsymbol{k}}^s}\right), \tag{22}$$

$$\sigma_{ab}^{(B,m)}(\omega) = \frac{e^2\tau}{\hbar(1-i\omega\tau)} \int [d\boldsymbol{k}]\left[\frac{\partial v_a^s}{\partial k_b}\left(\boldsymbol{m}_{\boldsymbol{k}}^s \cdot \boldsymbol{B}\right) - \frac{\partial\left(\boldsymbol{m}_{\boldsymbol{k}}^s \cdot \boldsymbol{B}\right)}{\partial k_a} v_b^s\right]\left(-\frac{\partial f_0^s}{\partial \varepsilon_{\boldsymbol{k}}^s}\right). \tag{23}$$

From Eq. (21), one finds readily the magnetoconductivity $\sigma_{ab}^{(B)}(\omega) = \sigma_{ba}^{(B)}(\omega)$. For the tilt $t_s = 0$, since the system possesses the time-reversal symmetry, $\sigma_{ab}^{(B)}(\omega)$ needs to obey the Onsager relation, and thus has to vanish [61,78,79]. However, when the tilt $t_s \neq 0$, the time-reversal symmetry is broken by the tilt, and so Eq. (21) can survive in the case of a tilted Weyl node. The first term in Eq. (21) [i.e., Eq. (22)] is related to the Berry curvature, and is reported previously (see, e.g., [27,31,32,80–83]). The second term in Eq. (21) [i.e., Eq. (23)] is our newly obtained result, and stems from the contribution of the orbital magnetic moment. In the following, the detailed analysis of Eq. (21) is given by considering the magnetic field perpendicular and parallel to the tilt axis.

(i) For the case of the magnetic field along the tilt direction($\boldsymbol{B} \parallel t_s$), the off-diagonal magnetoconductivity $\sigma_{ab}^{(B,\Omega)}(\omega)(a \neq b)$ vanishes since the integrands in Eqs. (22) and (23) contain product of an odd number of the velocity components. The diagonal component $\sigma_{aa}^{(B,\Omega)}(\omega)$ for small tilt parameter t_s reduces to

$$\sigma_{zz}^{(B,\Omega)}(\omega) = \sigma_1^{(B)} s\left[\frac{2\left(3-5t_s^2-3t_s^4\right)}{3t_s^3} + \frac{\left(t_s^2-1\right)^2}{t_s^4}\delta_s\right], \tag{24}$$

$$\sigma_{xx}^{(B,\Omega)}(\omega) = \sigma_1^{(B)} s\left[\frac{2t_s^2-3}{3t_s^3} - \frac{1-t_s^2}{2t_s^4}\delta_s\right], \tag{25}$$

where

$$\sigma_1^{(B)} = \frac{e^2\tau}{8\pi^2(1-i\omega\tau)}\frac{eB}{\hbar}\frac{v_F}{\hbar}, \tag{26}$$

and

$$\delta_s = \ln\left(\frac{1-t_s}{1+t_s}\right). \tag{27}$$

The results are in agreement with Ref. [27]. Via the similar calculation, Eq. (23) becomes

$$\sigma_{zz}^{(B,m)}(\omega) = \sigma_0^{(B)} s\left[\frac{2\left(-3+5t_s^2\right)}{3t_s^3} - \frac{\left(t_s^2-1\right)^2}{t_s^4}\delta_s\right], \tag{28}$$

$$\sigma_{xx}^{(B,m)}(\omega) = \sigma_0^{(B)} s\left[\frac{\left(3-8t_s^2\right)}{3t_s^3} - \frac{1-3t_s^2}{2t_s^4}\delta_s\right]. \tag{29}$$

(ii) For the case of the magnetic field perpendicular to the tilt direction ($\boldsymbol{B} \perp t_s$), the diagonal components of the conductivity vanish, and the off-diagonal components are given by [27]

$$\sigma_{xz}^{(B)}(\omega) = [\sigma^{(B,\Omega)} + \sigma^{(B,m)}]\cos\phi, \tag{30}$$

$$\sigma_{yz}^{(B)}(\omega) = [\sigma^{(B,\Omega)} + \sigma^{(B,m)}]\sin\phi, \tag{31}$$

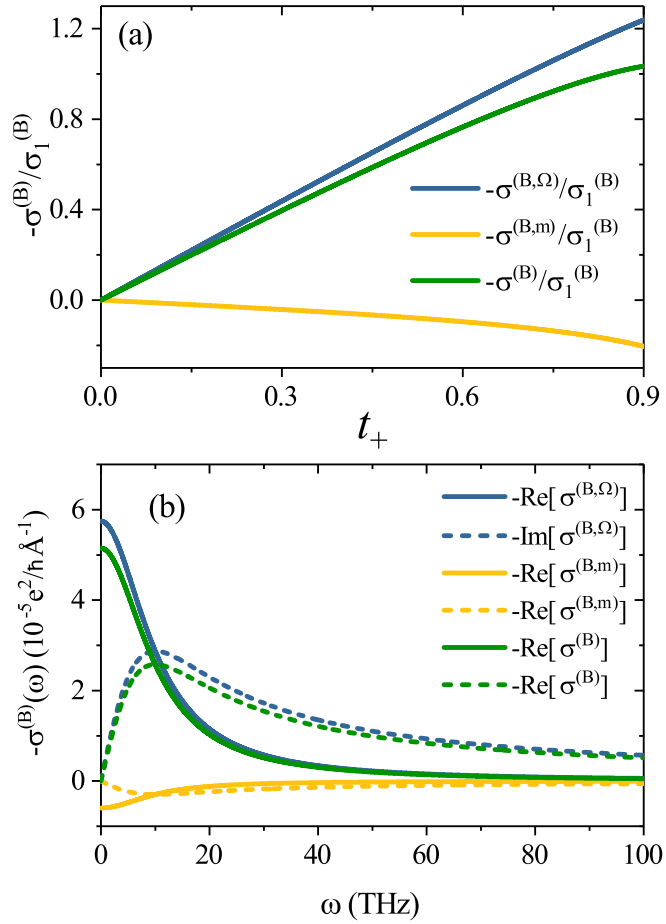

FIG. 2. (a) The dependence of the conductivity $\sigma^{(B)}(\omega)$ on the tilt t_+ [Eqs. (32) and (33)]. (b) The frequency dependence of the optical conductivity at $t_+ = 0.5$ and $B = 1$ T. The other parameters are the same as those of Fig. 1.

where $\phi = \arctan(B_y/B_x)$, $\sigma^{(B,\Omega)}$ and $\sigma^{(B,m)}$ are obtain from Eqs. (22) and (23), respectively,

$$\sigma^{(B,\Omega)} = \sigma_1^{(B)} s\left[\frac{-3+5t_s^2-6t_s^4}{3t_s^3} - \frac{\left(1-t_s^2\right)^2}{2t_s^4}\delta_s\right], \quad (32)$$

$$\sigma^{(B,m)} = \sigma_1^{(B)} s\left[-\frac{2t_s^2-3}{3t_s^3} + \frac{1-t_s^2}{2t_s^4}\delta_s\right]. \quad (33)$$

From Eqs. (24)–(33), we notice that the B-linear magnetoconductivity in tilted Weyl semimetals is independent of Fermi energy μ, and the odd function of t_s. According to the Nielsen-Ninomiya theorem [9,10], the Weyl nodes with opposite chirality always appear in pairs. The total magnetoconductivity of the system is the sum of all the Weyl nodes. Therefore, for the case of $t_+ = t_-$, where the tilt inversion symmetry is broken, the contribution of the Weyl node to the magnetoconductivity has the opposite sign for the opposite chirality, giving rise to $\sigma_{ab}^{(B)}(\omega) = 0$. Whereas, for the case of $t_+ = -t_-$, each Weyl node produces an identical contribution to the magnetoconductivity, and so the nonzero magnetoconductivity emerges for this case. Figure 2(a) shows the B-linear magnetoconductivity as a function of the tilt t_+. It is observed that the contribution from the orbital magnetic moment is always negative and decreases with increasing t_+, which partially cancels the contribution of the Berry curvature to magnetoconductivity. The total magnetoconductivity tends to slow down at the large t_+. Figure 2(b) shows the B-linear magnetoconductivity as a function of the THz incident light, we find that $\sigma^{(B)}(\omega)$ is about one order of magnitude greater than $\sigma^{(0)}(\omega)$. For a Weyl semimetal under an external magnetic field $B = 1$ T, the B-linear magnetoconductivity $\sigma_{ab}^{(B)}(\omega) \sim 10^2\ \Omega^{-1}\,\mathrm{m}^{-1}$ at $\omega \to 0$.

C. Quadratic-B contribution to the conductivity $\sigma_{ab}^{(B^2)}$

Substituting Eq. (14) into the first term of Eq. (15) and keeping terms to second order in $\boldsymbol{B}$, after straightforward but cumbersome algebra, we obtain the conductivity

$$\sigma_{ab}^{(B^2)}(\omega) = \sigma_{ab}^{(B^2,\Omega)}(\omega) + \sigma_{ab}^{(B^2,m)}(\omega), \quad (34)$$

where

$$\sigma_{ab}^{(B^2,\Omega)}(\omega) = \frac{e^4\tau}{\hbar^2(1-i\omega\tau)}\int[d\boldsymbol{k}]\Big[v_a^s v_b^s\big(\boldsymbol{B}\cdot\boldsymbol{\Omega}_{\boldsymbol{k}}^s\big)^2 - \big(v_a^s B_b + v_b^s B_a\big)\big(\boldsymbol{v}_{\boldsymbol{k}}^s\cdot\boldsymbol{\Omega}_{\boldsymbol{k}}^s\big)\big(\boldsymbol{B}\cdot\boldsymbol{\Omega}_{\boldsymbol{k}}^s\big) + B_a B_b\big(\boldsymbol{v}_{\boldsymbol{k}}^s\cdot\boldsymbol{\Omega}_{\boldsymbol{k}}^s\big)^2\Big]\left(-\frac{\partial f_0^s}{\partial\varepsilon_{\boldsymbol{k}}^s}\right), \quad (35)$$

$$\begin{aligned}\sigma_{ab}^{(B^2,m)}(\omega) = \frac{e^3\tau}{\hbar^2(1-i\omega\tau)}\int[d\boldsymbol{k}]\Bigg[&\frac{\partial}{\partial\boldsymbol{k}}\cdot\Big[v_a^s B_b\boldsymbol{\Omega}_{\boldsymbol{k}}^s\Big]\big(\boldsymbol{m}_{\boldsymbol{k}}^s\cdot\boldsymbol{B}\big) - \frac{\partial\Big[v_a^s\big(\boldsymbol{B}\cdot\boldsymbol{\Omega}_{\boldsymbol{k}}^s\big)\Big]}{\partial k_b}\big(\boldsymbol{m}_{\boldsymbol{k}}^s\cdot\boldsymbol{B}\big) + \frac{\partial\Big[B_a\big(\boldsymbol{v}_{\boldsymbol{k}}^s\cdot\boldsymbol{\Omega}_{\boldsymbol{k}}^s\big)\Big]}{\partial k_b}\big(\boldsymbol{m}_{\boldsymbol{k}}^s\cdot\boldsymbol{B}\big)\\ &+\frac{\partial\big(\boldsymbol{m}_{\boldsymbol{k}}^s\cdot\boldsymbol{B}\big)}{\partial k_a}\big(\boldsymbol{B}\cdot\boldsymbol{\Omega}_{\boldsymbol{k}}^s\big)v_b^s - \frac{\partial\big(\boldsymbol{m}_{\boldsymbol{k}}^s\cdot\boldsymbol{B}\big)}{\partial k_a}B_b\big(\boldsymbol{\Omega}_{\boldsymbol{k}}^s\cdot\boldsymbol{v}_{\boldsymbol{k}}^s\big) - \frac{\partial^2\big(\boldsymbol{m}_{\boldsymbol{k}}^s\cdot\boldsymbol{B}\big)}{e\partial k_a\partial k_b}\big(\boldsymbol{m}_{\boldsymbol{k}}^s\cdot\boldsymbol{B}\big) - B_a\frac{\partial\big(\boldsymbol{m}_{\boldsymbol{k}}^s\cdot\boldsymbol{B}\big)}{\partial\boldsymbol{k}}\cdot\boldsymbol{\Omega}_{\boldsymbol{k}}^s v_b^s\Bigg]\left(-\frac{\partial f_0^s}{\partial\varepsilon_{\boldsymbol{k}}^s}\right)\Bigg\}. \quad (36)\end{aligned}$$

$\sigma_{ab}^{(B^2,\Omega)}(\omega)$ and $\sigma_{ab}^{(B^2,m)}(\omega)$ arise from the contributions of the Berry-curvature $\boldsymbol{\Omega}_{\boldsymbol{k}}^s$ and the orbital magnetic moment $\boldsymbol{m}_{\boldsymbol{k}}^s$, respectively. In order to decode the information on $\boldsymbol{\Omega}_{\boldsymbol{k}}^s$ and $\boldsymbol{m}_{\boldsymbol{k}}^s$ in Eq. (34), we consider the two case in the following:

(i) In the case of $\boldsymbol{B} \parallel t_s$, one obtain the nonzero conductivity components [27]

$$\sigma_{zz}^{(B^2,\Omega)}(\omega) = 8\sigma_1^{(B^2)}, \quad (37)$$

$$\sigma_{xx}^{(B^2,\Omega)}(\omega) = \sigma_1^{(B^2)}, \quad (38)$$

where

$$\sigma_1^{(B^2)} = \frac{e^2\tau}{8\pi^2(1-i\omega\tau)}\left(\frac{eB}{\hbar}\right)^2\frac{\hbar v_F^3}{15\mu^2}. \quad (39)$$

Considering the effect of the orbital magnetic moment [see Eq. (36)], we have

$$\sigma_{zz}^{(B^2,m)}(\omega) = \left(-3+5t_s^2\right)\sigma_1^{(B^2)}, \quad (40)$$

$$\sigma_{xx}^{(B^2,m)}(\omega) = -\sigma_1^{(B^2)}. \quad (41)$$

Evidently, from Eqs. (38) and (41), $\sigma_{xx}^{(B^2,\Omega)}(\omega)$ and $\sigma_{xx}^{(B^2,m)}(\omega)$ have the opposite sign, thus the total conductivity $\sigma_{xx}^{(B^2)}(\omega)$ is equal to zero. For the conductivity component $\sigma_{zz}^{(B^2,m)}(\omega)$, there is a zero value point at $t_s = t_0 = (3/5)^{1/2}$. When $0 < t_s < t_0$(or $t_s > t_0$), $\sigma_{zz}^{(B^2,m)}(\omega) < 0$(or >0), so that the total conductivity is suppressed or enhanced on the left or right sides of t_0 by the orbital magnetic moment [see Fig. 3(a)].

(ii) In the case of $\boldsymbol{B} \perp t_s$, from Eq. (35), one obtain the diagonal components of the magnetoconductivities [27]

$$\sigma_{xx}^{(B^2,\Omega)}(\omega) = \left[\left(8+13t_s^2\right)\cos^2\phi + \sin^2\phi\right]\sigma_1^{(B^2)}, \quad (42)$$

$$\sigma_{zz}^{(B^2,\Omega)}(\omega) = \left(1+7t_s^2\right)\sigma_1^{(B^2)}, \quad (43)$$

and the off-diagonal components of the magnetoconductivities

$$\sigma_{xy}^{(B^2,\Omega)}(\omega) = \left(7+13t_s^2\right)\sin\phi\cos\phi\sigma_1^{(B^2)}. \quad (44)$$

Considering the effect of the orbital magnetic moment [see Eq. (36)], we have

$$\sigma_{xx}^{(B^2,m)}(\omega) = \left[\left(-3-6t_s^2\right)\cos^2\phi - \sin^2\phi\right]\sigma_1^{(B^2)}, \quad (45)$$

$$\sigma_{zz}^{(B^2,m)}(\omega) = \left(-1+t_s^2\right)\sigma_1^{(B^2)}, \quad (46)$$

$$\sigma_{xy}^{(B^2,m)}(\omega) = \left(-2-6t_s^2\right)\sin\phi\cos\phi\sigma_1^{(B^2)}. \quad (47)$$

It is noted that all the other magnetoconductivity components are zero. It is clear that the above conductivity equations are independent of chirality, i.e., the Weyl cones with opposite chiralities have the same contribution to the conductivity. Additionally, the conductivity component $\sigma_{xx}^{(B^2,m)}(\omega)$ is always negative [see Eq. (45)], a result that will leave the total conductivity $\sigma_{xx}^{(B^2)}(\omega)$ weakened. Likewise, the

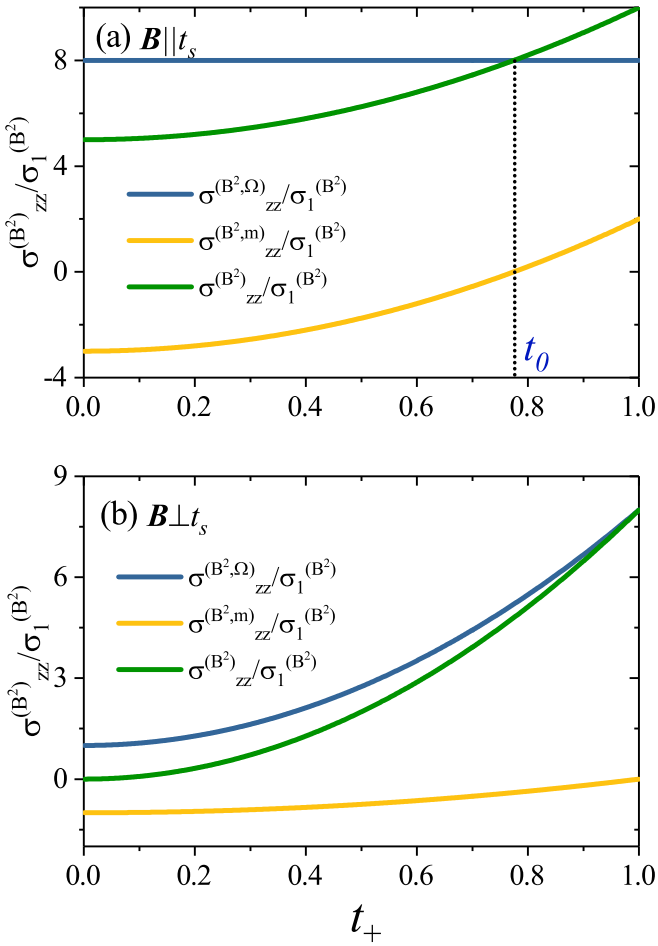

FIG. 3. The dependence of the conductivity $\sigma_{zz}^{(B^2)}(\omega)$ on the tilt t_+ for the case of (a) $\boldsymbol{B}||t_s$ [see Eqs. (37) and (40)], and (b) $\boldsymbol{B}\perp t_s$ [see Eqs. (43) and (46)].

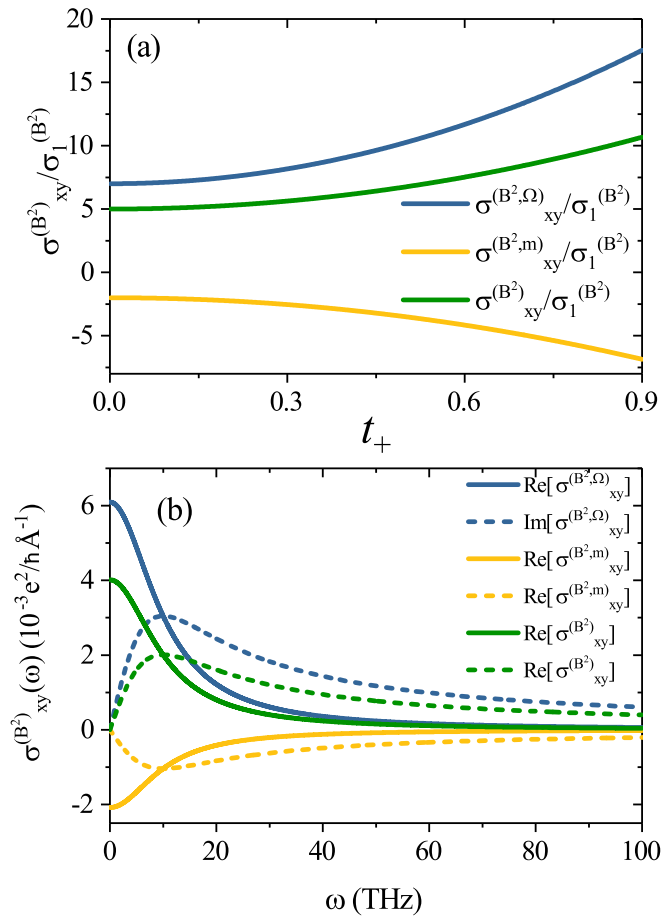

FIG. 4. (a) The dependence of planar Hall conductivity $\sigma_{xy}^{(B^2)}(\omega)$ on the tilt t_+ [see Eqs. (44) and (47)]. (b) The frequency dependence of optical conductivity at $t_+ = 0.5$, $\phi = \pi/4$, and $B = 1$ T. The other parameters are the same as those of Fig. 1.

orbital magnetic moment also leads to an attenuation of the conductivity component $\sigma_{zz}^{(B^2)}(\omega)$ [see Fig. 3(b)].

In the present system, the planar Hall effect can take place [24–29], and manifest itself in a nonzero conductivity $\sigma_{xy}^{(B^2)}(\omega)$. Similar to the diagonal component of the conductivity, $\sigma_{xy}^{(B^2)}(\omega)$ also consists of the contributions from the Berry curvature [Eq. (44)] and the orbital magnetic moment [Eq. (47)]. Figure 4(a) shows an effect of the tilt on the planar Hall magnetoconductivity. It is seen that the total planar Hall conductivity is suppressed when the orbit magnetic moment is present. Figure 4(b) shows the planar Hall magnetoconductivity as a function of the THz incident light at $\phi = \pi/4$, we find that $\sigma_{xy}^{(B^2)}(\omega)$ is about three orders of magnitude greater than $\sigma^{(0)}(\omega)$.

The B^2 dependence of the magnetoconductivity has been observed experimentally in the materials such as GdPtBi and TaP [28,29]. Recently, it is also shown that in the materials GdPtBi, a very strong planar Hall effect has been reported, which is due to the Berry curvature and chiral anomaly contributions [28]. Besides chiral anomaly, the planar Hall effect may be induced by the orbital magnetic moment [see Eq. (47)]. For the magnetic field $B \sim 2$ T, the dephasing rate $\gamma \sim 1$ meV, and $\mu \sim 30$ meV, we obtain the planar Hall resistivity $\rho_{xy}^{(B^2)}(\omega) \sim 1.0\ \mathrm{m\Omega\,cm}$ at $\omega = 2$ THz. These results are in agreement with the recent experimental findings [29], where a giant planar Hall effect is revealed in a nonmagnetic Weyl semimetal TaP with the large anisotropic orbital magnetoresistance.

D. Hall conductivities $\sigma_{ab}^{(H,0)}$ and $\sigma_{ab}^{(H,B)}$

The intrinsic Hall effect is engendered by the Berry curvature, as presented by the second term of Eq. (15), for which the further calculation gives

$$\sigma_{ab}^{H} = \sigma_{ab}^{(H,0)} + \sigma_{ab}^{(H,B)}, \tag{48}$$

where

$$\sigma_{ab}^{(H,0)} = -\frac{e^2}{\hbar}\epsilon_{abc}\int [d\boldsymbol{k}]\Omega_c^s f_0^s, \tag{49}$$

$$\sigma_{ab}^{(H,B)} = \frac{e^2}{\hbar}\epsilon_{abc}\int [d\boldsymbol{k}]\Omega_c^s(\boldsymbol{m}_{\boldsymbol{k}}^s\cdot\boldsymbol{B})\frac{\partial f_0^s}{\partial\varepsilon_{\boldsymbol{k}}^s}, \tag{50}$$

where ϵ_{abc} is the Levi-Civita symbol with $a, b, c, \in \{x, y, z\}$. The first term $\sigma_{ab}^{(H,0)}$ in Eq. (48), referring to the anomalous Hall effect, is not equivalent to zero only in the system with broken time-reversal symmetry [17,18]. While the second

term $\sigma_{ab}^{(H,B)}$ stands for the ordinary Hall conductivity linear in B, which is counterpart to a semiclassical description related to Landau level formation in the quantum limit [61].

We take the magnetic field $\boldsymbol{B} = (B\sin\theta\cos\phi, B\sin\theta\sin\phi, B\cos\theta)$ with $\theta = \arccos(B_z/B)$ and $\phi = \arctan(B_y/B_x)$. For a single Weyl node, the B-linear contribution to the Hall conductivity is expressed as

$$\sigma^{(H,B)} = \begin{pmatrix} 0 & \sigma_1^H\cos\theta & -\sigma_1^H\sin\theta\sin\phi \\ -\sigma_1^H\cos\theta & 0 & \sigma_1^H\sin\theta\cos\phi \\ \sigma_1^H\sin\theta\sin\phi & -\sigma_1^H\sin\theta\cos\phi & 0 \end{pmatrix}, \tag{51}$$

where

$$\sigma_1^H = -\frac{e^2}{\hbar}\frac{eB}{\hbar}\frac{\hbar v_F}{24\pi^2\mu}. \tag{52}$$

Clearly, the B-linear contribution to the Hall conductivity of Weyl semimetals does not depend on the tilt and the chirality of the valley, and is obtained by summing over all the Weyl nodes.

Besides, it is also emphatically mentioned that in the case of the weak magnetic field, a semiclassical description related to Landau level formation in the quantum limit shows that the Hall responses of Weyl semimetals under B is tied to the monopole physics in the momentum space described by the Berry curvature. Due to the linear dispersion relation in the Weyl semimetals, the Berry curvature is divergent at a Weyl node. Therefore, this leads to an inverse dependence of the linear Hall responses on μ, i.e., a divergence as μ goes to zero. Such a divergence of the Hall responses can be cut off by the energy broadening due to the nonzero relaxation time τ [61], which will incorporate a lower bound on the Fermi energy. A similar dependence on μ is also observed in the second-order nonlinear Hall responses (see below).

IV. SECOND-ORDER NONLINEAR RESPONSE OF WEYL SEMIMETALS

Next, we move on to the investigation for the second-order nonlinear magneto-optical response of Weyl semimetals. Substituting Eq. (7) into Eq. (8), neglecting the Lorentz force term, and retaining terms up to second order in $\boldsymbol{E}$, we obtain

$$\frac{1}{\hbar D}\left[-e\boldsymbol{E} - \frac{e^2}{\hbar}(\boldsymbol{E}\cdot\boldsymbol{B})\boldsymbol{\Omega}_{\boldsymbol{k}}^s\right]\cdot\frac{\partial\tilde{f}_1^s}{\partial\boldsymbol{k}} - i\omega\tilde{f}_2^s = -\frac{\tilde{f}_2^s}{\tau}. \tag{53}$$

A straightforward calculation results in

$$\tilde{f}_2^s = \frac{\tau}{1-2i\omega\tau}\frac{1}{\hbar D}\left[e\boldsymbol{E} + \frac{e^2}{\hbar}(\boldsymbol{E}\cdot\boldsymbol{B})\boldsymbol{\Omega}_{\boldsymbol{k}}^s\right]\cdot\frac{\partial\tilde{f}_1^s}{\partial\boldsymbol{k}}. \tag{54}$$

Inserting Eq. (13) into Eq. (54), and expanding it to first order in $\boldsymbol{B}$, we obtain

$$\begin{aligned}\tilde{f}_2^s = \frac{e\tau^2}{\hbar(1-2i\omega\tau)(1-i\omega\tau)}\Bigg\{&\boldsymbol{E}\cdot\frac{\partial}{\partial\boldsymbol{k}}\left[\left(e\boldsymbol{E} + \frac{e^2}{\hbar}(\boldsymbol{E}\cdot\boldsymbol{B})\boldsymbol{\Omega}_{\boldsymbol{k}}^s - \frac{e^2}{\hbar}(\boldsymbol{B}\cdot\boldsymbol{\Omega}_{\boldsymbol{k}}^s)\boldsymbol{E}\right)\cdot\boldsymbol{v}_{\boldsymbol{k}}^s\frac{\partial f_0^s}{\partial\varepsilon_{\boldsymbol{k}}^s} - \frac{e}{\hbar}\boldsymbol{E}\cdot\frac{\partial}{\partial\boldsymbol{k}}\left(\boldsymbol{m}_{\boldsymbol{k}}^s\cdot\boldsymbol{B}\frac{\partial f_0^s}{\partial\varepsilon_{\boldsymbol{k}}^s}\right)\right] \\ &+\left[\frac{e^2}{\hbar}(\boldsymbol{E}\cdot\boldsymbol{B})\boldsymbol{\Omega}_{\boldsymbol{k}}^s - \frac{e^2}{\hbar}(\boldsymbol{B}\cdot\boldsymbol{\Omega}_{\boldsymbol{k}}^s)\boldsymbol{E}\right]\cdot\frac{\partial}{\partial\boldsymbol{k}}\left(\boldsymbol{E}\cdot\boldsymbol{v}_{\boldsymbol{k}}^s\frac{\partial f_0^s}{\partial\varepsilon_{\boldsymbol{k}}^s}\right)\Bigg\}.\end{aligned} \tag{55}$$

Now the electric current density at the frequency 2ω is given by

$$\boldsymbol{j}_2 = -e\int[d\boldsymbol{k}]\left[\tilde{\boldsymbol{v}}_{\boldsymbol{k}}^s + \frac{e}{\hbar}(\tilde{\boldsymbol{v}}_{\boldsymbol{k}}^s\cdot\boldsymbol{\Omega}_{\boldsymbol{k}}^s)\boldsymbol{B}\right]\tilde{f}_2^s - \frac{e^2}{\hbar}\int[d\boldsymbol{k}]\boldsymbol{E}\times\boldsymbol{\Omega}_{\boldsymbol{k}}^s\tilde{f}_1^s. \tag{56}$$

According to the definition of second harmonic conductivity, this equation should be written in the form

$$\boldsymbol{j}(2\omega) = \sigma(2\omega)\boldsymbol{E}(\omega)\boldsymbol{E}(\omega), \tag{57}$$

where $\sigma(2\omega)$ is the second harmonic conductivity.

A. The second harmonic conductivity $\sigma_{abc}^{(0)}$ in absence of magnetic field

In this subsection, we calculate the second harmonic current of the Weyl semimetals system in absence of magnetic fields. When $\boldsymbol{B} = 0$, substituting Eq. (55) into the first term of Eq. (56), the second harmonic conductivity tensor can be obtained:

$$\sigma_{abc}^{(0)}(2\omega) = \frac{e^3\tau^2}{\hbar(1-2i\omega\tau)(1-i\omega\tau)}\int[d\boldsymbol{k}]\frac{\partial v_a}{\partial k_c}v_b\frac{\partial f_0^s}{\partial\varepsilon_{\boldsymbol{k}}^s}, \tag{58}$$

we find that the aaz, aza, and zaa ($a = x, y, z$) components of the second harmonic conductivity tensor are nonzero and all other components equal to zero [77]:

$$\sigma_{zzz}^{(0)}(2\omega) = 2\sigma_{DL}\left[\frac{-6+4t_s^2}{t_s^3} - \frac{3(1-t_s^2)}{t_s^4}\delta_s\right], \tag{59}$$

$$\sigma_{xxz}^{(0)}(2\omega) = \sigma_{DL}\left[\frac{6}{t_s^3} + \frac{3-t_s^2}{t_s^4}\delta_s\right], \tag{60}$$

where the Drude-like frequency dependent complex conductivity is

$$\sigma_{DL} = \frac{e^3\tau^2\mu}{8\pi^2\hbar^3(1-2i\omega\tau)(1-i\omega\tau)}. \tag{61}$$

The second harmonic conductivity tensor satisfies the relation $\sigma_{zxx}^{(0)}(2\omega) = \sigma_{zyy}^{(0)}(2\omega) = \sigma_{xzx}^{(0)}(2\omega) = \sigma_{yzy}^{(0)}(2\omega) = \sigma_{xxz}^{(0)}(2\omega) = \sigma_{yyz}^{(0)}(2\omega)$, and it does not depend on the chirality of Weyl node. The total second harmonic conductivity in tilted Weyl semimetals is the sum of a pair of Weyl nodes. For the case with tilt inversion symmetry ($t_+ = -t_-$), $\sigma_{abc}^{(0)}(2\omega) = 0$. For the case with broken tilt inversion symmetry ($t_+ = t_-$), the conductivity $\sigma_{abc}^{(0)}(2\omega) \neq 0$.

From Fig. 5(a), it is important to see that the $\sigma_{abc}^{(0)}(2\omega)$ becomes exactly zero when $t_s \to 0$. The presence of the tilt

makes the Weyl semimetals with ellipsoidal Fermi surface, thus the tilt performs a very important function to get the second harmonic generation in Weyl semimetals [77]. And it is clear that $\sigma^{(0)}_{zzz}(\omega)$ is more sensitive to tilt than $\sigma^{(0)}_{xxz}(\omega)$ [see Fig. 5(a)]. Different from the linear response regime [Figs. 1(b), 2(b), and 4(b)], the real parts of $\sigma^{(0)}_{abc}(2\omega)$ exhibit positive and negative amplitudes because of the complex denominator function σ_{DL} contribution to the second harmonic generation processes [Fig. 5(b)]. Adopting a laser frequency $\omega \sim 2$ THz, the electric field strength $\sim 10^4$ V/m, and a laser spot size of 50-μm diameter in a Weyl semimetal, we obtain the nonlinear current $\sim 10^{-5}$ A. The nonlinear optical polarizability $\chi^{(0)}(2\omega)$ for the process of the second harmonic generation is given by $\chi^{(0)}(2\omega) = \sigma^{(0)}(2\omega)/2i\omega\epsilon_0$, where ϵ_0 is vacuum permittivity, we find $\chi^{(0)}(2\omega) \sim 10^3$ pm/V. These results are consistent with the experimental results [47].

B. B-linear contribution to the second harmonic conductivity $\sigma^{(B)}_{abc}$

In the presence of the magnetic field, inserting Eq. (55) into the first term of Eq. (56), we derive the B-linear contribution to the second harmonic conductivity

$$\sigma^{(B)}_{abc}(2\omega) = \frac{e^3\tau^2}{\hbar(1-2i\omega\tau)(1-i\omega\tau)}\int[d\boldsymbol{k}]\Big\{\frac{\partial v^s_a}{\partial k_c}\Big[-\frac{eB_b}{\hbar}\big(\boldsymbol{v}^s_{\boldsymbol{k}}\cdot\boldsymbol{\Omega}^s_{\boldsymbol{k}}\big)+\frac{ev^s_b}{\hbar}\big(\boldsymbol{B}\cdot\boldsymbol{\Omega}^s_{\boldsymbol{k}}\big)\Big]-\frac{eB_c}{\hbar}\frac{\partial}{\partial\boldsymbol{k}}\cdot\big(v^s_a\boldsymbol{\Omega}^s_{\boldsymbol{k}}\big)v^s_b$$
$$+\frac{e}{\hbar}\frac{\partial\big[v^s_a\big(\boldsymbol{B}\cdot\boldsymbol{\Omega}^s_{\boldsymbol{k}}\big)\big]}{\partial k_c}v^s_b-\frac{eB_a}{\hbar}\frac{\partial\big(\boldsymbol{v}^s_{\boldsymbol{k}}\cdot\boldsymbol{\Omega}^s_{\boldsymbol{k}}\big)}{\partial k_c}v^s_b+\frac{\partial^2\big(\boldsymbol{m}^s_{\boldsymbol{k}}\cdot\boldsymbol{B}\big)}{\hbar\partial k_a\partial k_c}v^s_b-\frac{\partial^2 v^s_a}{\hbar\partial k_b\partial k_c}\big(\boldsymbol{m}^s_{\boldsymbol{k}}\cdot\boldsymbol{B}\big)\Big\}\Big(-\frac{\partial f^s_0}{\partial\varepsilon^s_{\boldsymbol{k}}}\Big). \tag{62}$$

The analysis of Eq. (62) is carried out by considering the following two different cases:

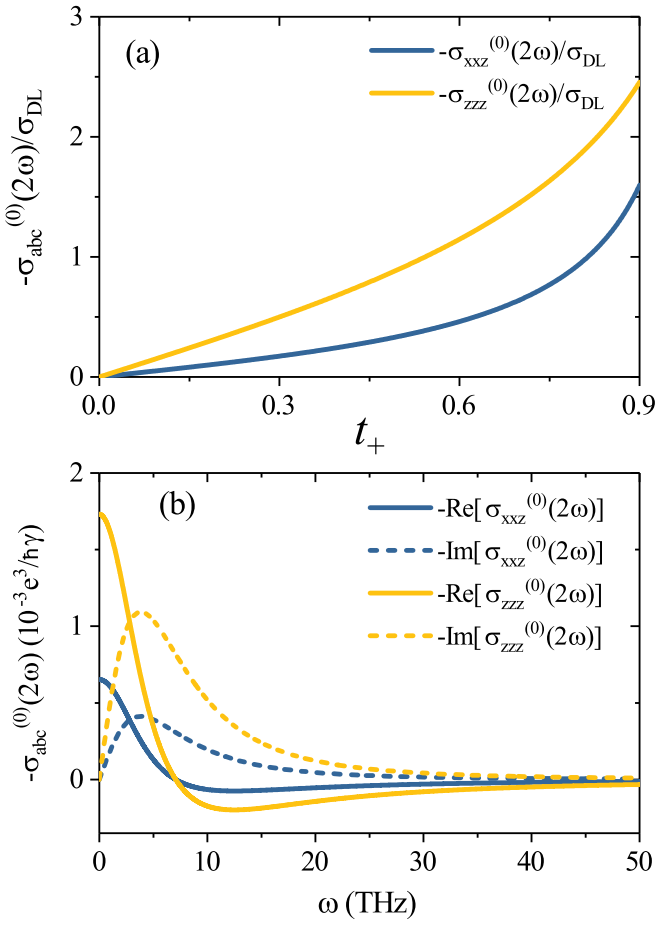

FIG. 5. (a) The nonlinear conductivities for the process of second harmonic generation as a function of the tilt t_+ [see Eqs. (59) and (60)]. (b) The frequency dependence of optical conductivities at $t_+ = 0.5$. Here the relaxation rate $\gamma = \hbar/\tau$. The other parameters are the same as those of Fig. 1.

(i) In the case of $B \parallel t_s$, for a single Weyl node, we obtain the magnetoconductivity components

$$\sigma^{(B)}_{xzx}(2\omega) = s\tfrac{2}{3}\sigma^{(B)}_2, \tag{63}$$

$$\sigma^{(B)}_{zxx}(2\omega) = -s\tfrac{2}{3}\sigma^{(B)}_2, \tag{64}$$

where

$$\sigma^{(B)}_2 = \frac{e^3\tau^2}{8\pi^2\hbar(1-2i\omega\tau)(1-i\omega\tau)}\frac{eB}{\hbar}\frac{v_F^2}{\mu}. \tag{65}$$

We note that the other nonzero second harmonic conductivity components satisfy the relations: $\sigma^{(B)}_{xzx}(2\omega) = \sigma^{(B)}_{yzy}(2\omega)$, $\sigma^{(B)}_{zxx}(2\omega) = \sigma^{(B)}_{zyy}(2\omega)$.

(ii) In the case of $B \perp t_s$, we get the nonzero conductivity components

$$\sigma^{(B)}_{zxz}(2\omega) = s\tfrac{2}{3}\sigma^{(B)}_2\cos\phi, \tag{66}$$

$$\sigma^{(B)}_{xzz}(2\omega) = -s\tfrac{2}{3}\sigma^{(B)}_2\cos\phi, \tag{67}$$

$$\sigma^{(B)}_{zyz}(2\omega) = s\tfrac{2}{3}\sigma^{(B)}_2\sin\phi, \tag{68}$$

$$\sigma^{(B)}_{yzz}(2\omega) = -s\tfrac{2}{3}\sigma^{(B)}_2\sin\phi. \tag{69}$$

The above equation shows that the B-linear contribution to the second harmonic conductivity is dependent of the chirality but independent of the tilt. Summing the conductivity over the Weyl cones with opposite chirality cancels each other, leading to the disappearance of the total B-linear contribution to the second harmonic conductivity.

C. The second-order nonlinear Hall conductivity $\sigma^{(H,0)}_{abc}$ in absence of magnetic field

In this subsection, we study the second-order nonlinear Hall effect of Weyl semimetals in absence of magnetic field. Inserting Eq. (14) into the second term in Eq. (56) and taking $\boldsymbol{B} = 0$, we obtain the nonlinear Hall conductivity.

$$\sigma^{(H,0)}_{abc} = \epsilon_{acd}\frac{e^3\tau}{\hbar^2(1-i\omega\tau)}D_{bd} \tag{70}$$

which is determined by the so-called Berry dipole [48]

$$D_{bd} = \int [d\boldsymbol{k}]\Omega_d^s \hbar v_b^s \left(-\frac{\partial f_0^s}{\partial \varepsilon_{\boldsymbol{k}}^s}\right). \tag{71}$$

The further calculation shows that the nonzero components of the Berry dipole moment are

$$D_{xx} = D_{yy} = -s\frac{1}{16\pi^2}\left(\frac{2}{t_s^2} + \frac{1-t_s^2}{t_s^3}\ln\frac{1-t_s}{1+t_s}\right), \tag{72}$$

$$D_{zz} = -s\frac{1}{8\pi^2}\frac{t_s^2-1}{t_s^3}\left(2t_s + \ln\frac{1-t_s}{1+t_s}\right). \tag{73}$$

From the above equations, One can notice that the Berry dipole moment is dependent of the chirality, and an even function of the tilt. Therefore, contributions from a pair of Weyl nodes with opposite chirality exactly cancel each other [55,56]. However, several Weyl semimetals without spatial inversion symmetry are accompanied by the enhancement of the Berry curvature dipole, which allows to measure the finite second-harmonic Hall voltage [49–54].

From Eqs. (72) and (73), the Berry dipole moment is independent of the chemical potential μ. The reason for this is that due to the intrinsic properties of the electronic structure of the Weyl semimetals, the Berry curvature becomes dependent of $1/k^2$. Accordingly, the integral over the momentum k in Eq. (71) is only determined by the topology of the Weyl nodes, which leads to this result unrelated to μ [55].

D. *B*-linear contribution to the second-order nonlinear Hall conductivity $\sigma_{abc}^{(H,B)}$

Now, we focus on the second-order nonlinear Hall effect in a weak magnetic field. Inserting Eq. (14) into the second term of Eq. (56), the B-linear dependent complex nonlinear Hall conductivity is then given by

$$\sigma_{abc}^{(H,B)} = \epsilon_{acd}\frac{e^3\tau}{\hbar^2(1-i\omega\tau)}\left[D_{bd}^{\Omega} + D_{bd}^{m}\right]. \tag{74}$$

with

$$D_{bd}^{\Omega} = \int [d\boldsymbol{k}] e\Omega_d^s\left[B_b\left(\boldsymbol{\Omega}_{\boldsymbol{k}}^s\cdot\boldsymbol{v}_{\boldsymbol{k}}^s\right) - v_b^s\left(\boldsymbol{B}\cdot\boldsymbol{\Omega}_{\boldsymbol{k}}^s\right)\right]\left(-\frac{\partial f_0^s}{\partial \varepsilon_{\boldsymbol{k}}}\right), \tag{75}$$

$$D_{bd}^{m} = \int [d\boldsymbol{k}]\frac{\partial\Omega_d^s}{\partial k_b}\left(\boldsymbol{m}_{\boldsymbol{k}}^s\cdot\boldsymbol{B}\right)\left(-\frac{\partial f_0^s}{\partial \varepsilon_{\boldsymbol{k}}}\right), \tag{76}$$

where D_{bd}^{Ω} and D_{bd}^{m} are the contributions induced by the Berry-curvature and the orbital magnetic moment, respectively.

(i) In the case of $B \parallel t_s$, the nonzero components are

$$D_{xx}^{\Omega} = D_{yy}^{\Omega} = -t_s D_2^{(B)}, \tag{77}$$

$$D_{zz}^{\Omega} = 2t_s D_2^{(B)}, \tag{78}$$

and

$$D_{xx}^{m} = D_{yy}^{m} = 2t_s D_2^{(B)}, \tag{79}$$

$$D_{zz}^{m} = -4t_s D_2^{(B)}. \tag{80}$$

where

$$D_2^{(B)} = \frac{1}{8\pi^2}\frac{eB}{\hbar}\frac{\hbar^2 v_F^2}{15\mu^2}. \tag{81}$$

(ii) In the case of $B \perp t_s$, we obtain

$$D_{zx}^{\Omega} = -6t_s D_2^{(B)}\cos\phi, \tag{82}$$

$$D_{xz}^{\Omega} = 9t_s D_2^{(B)}\cos\phi, \tag{83}$$

$$D_{zy}^{\Omega} = -6t_s D_2^{(B)}\sin\phi, \tag{84}$$

$$D_{yz}^{\Omega} = 9t_s D_2^{(B)}\sin\phi, \tag{85}$$

and

$$D_{zx}^{m} = -3t_s D_2^{(B)}\cos\phi, \tag{86}$$

$$D_{zy}^{m} = -3t_s D_2^{(B)}\sin\phi. \tag{87}$$

It is noted that $D_{zx}^{m} = D_{xz}^{m}$ and $D_{zy}^{m} = D_{yz}^{m}$, and all other components equal to zero.

The nonlinear Hall effect can be modulated by the polarization of the incident light, as discussed below. Using Eq. (74), the electric current is rewritten in the form of

$$\boldsymbol{j}(2\omega) = \frac{e^3\tau}{\hbar^2(1-i\omega\tau)}(\hat{D}\cdot\boldsymbol{E})\times\boldsymbol{E}. \tag{88}$$

Here it is assumed that an electromagnetic wave travels in the x direction:

$$\boldsymbol{E}(\boldsymbol{r},t) = |\boldsymbol{E}(\omega)|\mathrm{Re}[|\psi\rangle e^{-i\omega t+iqx}], \tag{89}$$

where

$$|\psi\rangle \overset{\text{def}}{=} \begin{pmatrix}\psi_y\\ \psi_z\end{pmatrix} = \begin{pmatrix}\sin\theta e^{i\alpha_y}\\ \cos\theta e^{i\alpha_z}\end{pmatrix} \tag{90}$$

is the Jones vector in the $y-z$ plane with phases α_y, α_z, and the amplitudes $E_y = |\boldsymbol{E}|\sin\theta$ and $E_z = |\boldsymbol{E}|\cos\theta$. Substituting Eq. (89) in Eq. (88), we obtain the nonlinear Hall current

$$j_x(2\omega) = \frac{e^3\tau}{\hbar^2(1-i\omega\tau)}\frac{D_{yy}^{(B)} - D_{zz}^{(B)}}{2}\sin 2\theta e^{i(\alpha_y+\alpha_z)}|\boldsymbol{E}|^2, \tag{91}$$

whose real and imaginary parts are related to the phases of incident light [see Eq. (91)]. For simplicity, we take $\alpha_y = \alpha_z = 0$. Equation (91) is rewritten as σ_{xzy} through $j_x = \sigma_x E_y E_z = \sigma_{xyz}E_y E_z + \sigma_{xzy}E_y E_z \sim (D_{yy} - D_{zz})E_y E_z$. Whence, for one Weyl node we have

$$\sigma_x^{(H,B)}(2\omega) = \frac{e^3\tau}{\hbar^2(1-i\omega\tau)}\frac{3t_s}{2}D_2^{(B)}\sin 2\theta. \tag{92}$$

In contrast to the case of $B = 0$, the B-linear contribution to the nonlinear Hall conductivity is independent of the chirality, and the odd function of t_s. Only in the system with broken tilt inversion symmetry ($t_+ = t_-$), the conductivity $\sigma_x(2\omega) \neq 0$. From Eq. (92), evidently, $\sigma_x(2\omega)$ reaches its maximum when the polarization direction $\theta = \pm\pi/4$ and vanishes at $\theta = 0, \pi/2$, as further reflected in Fig. 6(b). Taking the parameters $\omega \sim 5$ THz, $|\boldsymbol{E}| \sim 10^4$ V/m, and a laser spot size of 50-μm diameter in a Weyl semimetal, we estimate the nonlinear current $j_x(2\omega) \sim 1.65\times 10^{-3}$ A, and the nonlinear

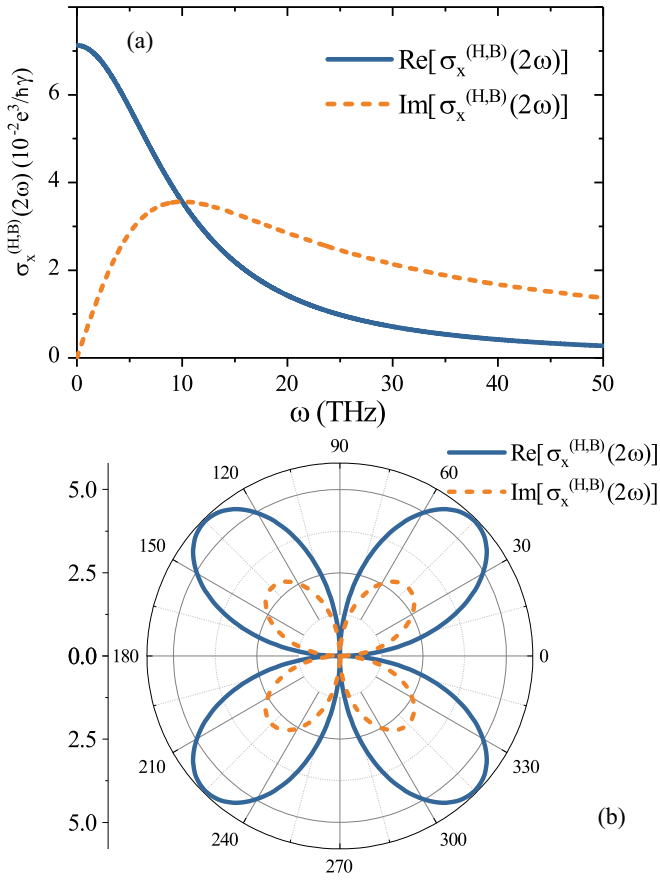

FIG. 6. (a) The nonlinear Hall conductivity $\sigma_x(2\omega)$ for the process of second harmonic generation as a function of the incident photon frequency at $t_+ = 0.5$, $B = 1$ T, and $\theta = \pi/4$ [see Eq. (92)]. (b) The angle dependence of the nonlinear Hall conductivity at $\omega = 5$ THz. The other parameters are the same as those of Fig. 1.

optical polarizability $\chi^{(B)}(2\omega) \sim 10^4$ pm/V. It is suggested that the Weyl semimetals is an interesting nonlinear optical media in a wide range of frequency.

V. CONCLUSION

We have presented a systematic investigation of the linear and nonlinear magneto-optical responses in tilted Weyl semimetals, derive an analytic expression for the magnetoconductivity by using the Boltzmann equation method, and find that: (i) In the linear response regime, there is a Drude-type conductivity from each Weyl node. In the absence of a magnetic field, the optical conductivity is sensitive to the tilt owing to the anisotropy of the drift velocities in the Weyl semimetals. When the magnetic field is applied, in the tilted Weyl node, the B-linear conductivity consists of two contributions, one from the Berry curvature and the other from the orbital magnetic moment. These two contributions partly cancel each other, leading to the suppression of the total conductivities. (ii) In the second-order nonlinear response regime, without a magnetic field, an analytical formula for the second harmonic conductivity is derived, showing chirality independence. In the presence of the magnetic field, the B-linear second harmonic conductivities in a single Weyl cone neither vanish, nor rely on the tilt. But the diagonal conductivities from two Weyl nodes with opposite chirality cancel each other, while the off-diagonal (Hall) conductivities are also derived, where these two contributions of Berry-curvature and orbital magnetic moment partly cancel.

ACKNOWLEDGMENTS

Y.G. is supported by University-level key projects of Anhui University of science and technology (Grant No. xjzd2020-12), and the Natural Science Foundation of Anhui Province University (Grant No. KJ2021A0415). Z.Q.Z and H.J. are supported by the National Basic Research Program of China (Grant No. 2019YFA0308403), NSFC under Grant No. 12147126 and No. 11822407. K.H.D. is supported by the Scientific Research Fund of Hunan Provincial Education Department (Grant No. 18K051), and the Construct Program of the Key Discipline of Hunan Province.

APPENDIX A: SOME USEFUL FORMULAS

In this Appendix we present the formulas used in the main text. The semiclassical expression of the velocity for the band energy $\varepsilon^s_{\boldsymbol{k}}$, and its differentiation are listed as follows:

$$v^s_{\boldsymbol{k}} = \frac{1}{\hbar}\frac{\partial \varepsilon^s_{\boldsymbol{k}}}{\partial \boldsymbol{k}} = v_F\left(t_s \hat{\boldsymbol{e}}_z + \frac{\boldsymbol{k}}{k}\right), \tag{A1}$$

$$\frac{\partial v^s_a}{\partial k_b} = v_F \frac{k^2\delta_{ab} - k_a k_b}{k^3}, \tag{A2}$$

$$\frac{\partial v^s_a}{\partial k_b \partial k_c} = v_F\left(\frac{3k_a k_b k_c}{k^5} - \frac{k_a\delta_{bc} + k_b\delta_{ac} + k_c\delta_{ab}}{k^3}\right). \tag{A3}$$

The Berry curvature and the differentiation are given by

$$\Omega^s_a = -s\frac{k_a}{2k^3}, \tag{A4}$$

$$\frac{\partial \Omega^s_a}{\partial k_b} = s\frac{3k_a k_b - k^2\delta_{ab}}{2k^5}. \tag{A5}$$

The orbital magnetic moment and the differentiation are expressed as

$$m^s_a = -s\frac{ev_F k_a}{2k^2}, \tag{A6}$$

$$\frac{\partial m^s_a}{\partial k_b} = sev_F\frac{2k_a k_b - k^2\delta_{ab}}{2k^4}, \tag{A7}$$

$$\frac{\partial m^s_a}{\partial k_b \partial k_c} = sev_F\left(\frac{k_a\delta_{bc} + k_b\delta_{ac} + k_c\delta_{ab}}{k^4} - \frac{4k_a k_b k_c}{k^6}\right). \tag{A8}$$

APPENDIX B: DETAILS OF THE CALCULATIONS USING SPHERICAL POLAR COORDINATES

In this paper, we focus on the n-doped Weyl semimetals with a positive chemical potential μ. In general, one can decompose the momentum $\boldsymbol{k}$ into parallel and perpendicular parts:

$$k_x = k\sin\theta\cos\phi, \tag{B1}$$

$$k_y = k\sin\theta\sin\phi, \tag{B2}$$

$$k_z = k\cos\theta. \tag{B3}$$

As an example, we calculate the second harmonic conductivity component $\sigma^{(0)}_{zzz}(2\omega)$ in absence of a magnetic field,

$$\begin{aligned}\sigma^{(0)}_{zzz}(2\omega) &= -\frac{e^3\tau^2}{\hbar(1-2i\omega\tau)(1-i\omega\tau)}\int[d\boldsymbol{k}]\frac{\partial v_z}{\partial k_z}v_z\left(-\frac{\partial f^s_0}{\partial\varepsilon_{\boldsymbol{k}}}\right)\\ &= -\frac{e^3\tau^2}{\hbar(1-2i\omega\tau)(1-i\omega\tau)}\int[d\boldsymbol{k}]v_F\frac{k_x^2+k_y^2}{k^3}\\ &\quad\times v_F\left(t_s+\frac{k_z}{k}\right)\left(-\frac{\partial f^s_0}{\partial\varepsilon_{\boldsymbol{k}}}\right)\\ &= -\frac{e^3\tau^2}{8\pi^3\hbar(1-2i\omega\tau)(1-i\omega\tau)}\int k^2\sin\theta dk d\theta d\phi\\ &\quad\times v_F\frac{\sin^2\theta\cos^2\phi+\sin^2\theta\sin^2\phi}{k}v_F(t_s+\cos\theta)\\ &\quad\times\delta[\hbar v_F k(1+t_s\cos\theta)-\mu]\\ &= \sigma_{DL}\int\sin\theta d\theta\frac{-\sin^2\theta}{(1+t_s\cos\theta)^2}(t_s+\cos\theta)\\ &= \sigma_{DL}\int_{-1}^{1}dx\frac{-(1-x^2)(t_s+x)}{(1+t_sx)^2}\\ &= 2\sigma_{DL}\left[\frac{-6+4t_s^2}{t_s^3}-\frac{3(1-t_s^2)}{t_s^4}\ln\frac{1-t_s}{1+t_s}\right],\end{aligned}$$

where the Drude-like frequency dependent complex conductivity is

$$\sigma_{DL}=\frac{e^3\tau^2\mu}{8\pi^2\hbar^3(1-2i\omega\tau)(1-i\omega\tau)}. \tag{B4}$$

[1] S. Murakami, Phase transition between the quantum spin Hall and insulator phases in 3D: Emergence of a topological gapless phase, New J. Phys. **9**, 356 (2007).

[2] X. Wan, A. M. Turner, A. Vishwanath, and S. Y. Savrasov, Topological semimetal and Fermi-arc surface states in the electronic structure of pyrochlore iridates, Phys. Rev. B **83**, 205101 (2011).

[3] K. Y. Yang, Y. M. Lu, and Y. Ran, Quantum Hall effects in a Weyl semimetal: Possible application in pyrochlore iridates, Phys. Rev. B **84**, 075129 (2011).

[4] A. A. Burkov and L. Balents, Weyl Semimetal in a Topological Insulator Multilayer, Phys. Rev. Lett. **107**, 127205 (2011).

[5] G. Xu, H. Weng, Z. Wang, X. Dai, and Z. Fang, Chern Semimetal and the Quantized Anomalous Hall Effect in $HgCr_2Se_4$, Phys. Rev. Lett. **107**, 186806 (2011).

[6] S.-M. Huang, S.-Y. Xu, I. Belopolski, C.-C. Lee, G. Chang, B. Wang, N. Alidoust, G. Bian, M. Neupane, C. Zhang *et al.*, A Weyl Fermion semimetal with surface Fermi arcs in the transition metal monopnictide TaAs class, Nat. Commun. **6**, 7373 (2015).

[7] B. Q. Lv, N. Xu, H. M. Weng, J. Z. Ma, P. Richard, X. C. Huang, L. X. Zhao, G. F. Chen, C. E. Matt, F. Bisti *et al.*, Observation of Weyl nodes in TaAs, Nat. Phys. **11**, 724 (2015).

[8] S.-Y. Xu, I. Belopolski, N. Alidoust, M. Neupane, G. Bian, C. Zhang, R. Sankar, G. Chang, Z. Yuan, C.-C. Lee *et al.*, Discovery of a Weyl fermion semimetal and topological Fermi arcs, Science **349**, 613 (2015).

[9] H. B. Nielsen and M. Ninomiya, Absence of neutrinos on a lattice: (I). Proof by homotopy theory, Nucl. Phys. B **185**, 20 (1981).

[10] H. B. Nielsen and M. Ninomiya, Absence of neutrinos on a lattice: (II). Intuitive topological proof, Nucl. Phys. B **193**, 173 (1981).

[11] T. Timusk, J. P. Carbotte, C. C. Homes, D. N. Basov, and S. G. Sharapov, Three-dimensional Dirac fermions in quasicrystals as seen via optical conductivity, Phys. Rev. B **87**, 235121 (2013).

[12] M. Orlita, D. M. Basko, M. S. Zholudev, F. Teppe, W. Knap, V. I. Gavrilenko, N. N. Mikhailov, S. A. Dvoretskii, P. Neugebauer, C. Faugeras *et al.*, Observation of three-dimensional massless Kane fermions in a zinc-blende crystal, Nat. Phys. **10**, 233 (2014).

[13] A. A. Zyuzin and A. A. Burkov, Topological response in Weyl semimetals and the chiral anomaly, Phys. Rev. B **86**, 115133 (2012).

[14] D. T. Son and N. Yamamoto, Berry Curvature, Triangle Anomalies, and the Chiral Magnetic Effect in Fermi Liquids, Phys. Rev. Lett. **109**, 181602 (2012).

[15] D. T. Son and B. Z. Spivak, Chiral anomaly and classical negative magnetoresistance of Weyl metals, Phys. Rev. B **88**, 104412 (2013).

[16] P. E. C. Ashby and J. P. Carbotte, Chiral anomaly and optical absorption in Weyl semimetals, Phys. Rev. B **89**, 245121 (2014).

[17] D. Xiao, M. C. Chang, and Q. Niu, Berry phase effects on electronic properties, Rev. Mod. Phys. **82**, 1959 (2010).

[18] N. Nagaosa, J. Sinova, S. Onoda, A. H. MacDonald, and N. P. Ong, Anomalous Hall effect, Rev. Mod. Phys. **82**, 1539 (2010).

[19] J. Hu, J. Y. Liu, D. Graf, S. M. A. Radmanesh, D. J. Adams, A. Chuang, Y. Wang, I. Chiorescu, J. Wei, L. Spinu, and Z. Q. Mao, π Berry phase and Zeeman splitting of Weyl semimetal tap, Sci. Rep. **6**, 18674 (2016).

[20] F. Arnold, C. Shekhar, S.-C. Wu, Y. Sun, R. D. dos Reis, N. Kumar, M. Naumann, M. O. Ajeesh, M. Schmidt, A. G. Grushin *et al.*, Negative magnetoresistance without well-defined chirality in the Weyl semimetal tap, Nat. Commun. **7**, 11615 (2016).

[21] Y. Li, Z. Wang, P. Li, X. Yang, Z. Shen, F. Sheng, X. Li, Y. Lu, Y. Zheng, and Z.-A. Xu, Negative magnetoresistance in Weyl semimetals NbAs and Nbp: Intrinsic chiral anomaly and extrinsic effects, Front. Phys. **12**, 127205 (2017).

[22] Sudesh, P. Kumar, P. Neha, T. Das, and S. Patnaik, Evidence for trivial Berry phase and absence of chiral anomaly in semimetal NbP, Sci. Rep. **7**, 46062 (2017).

[23] A. C. Niemann, J. Gooth, S.-C. Wu, S. Bäßler, P. Sergelius, R. Hühne, B. Rellinghaus, C. Shekhar, V. Süß, M. Schmidt *et al.*, Chiral magnetoresistance in the Weyl semimetal NbP, Sci. Rep. **7**, 43394 (2017).

[24] A. A. Burkov, Giant planar Hall effect in topological metals, Phys. Rev. B **96**, 041110(R) (2017).

[25] S. Nandy, G. Sharma, A. Taraphder, and S. Tewari, Chiral Anomaly as the Origin of the Planar Hall Effect in Weyl Semimetals, Phys. Rev. Lett. **119**, 176804 (2017).

[26] D. Ma, H. Jiang, H. Liu, and X. C. Xie, Planar Hall effect in tilted Weyl semimetals, Phys. Rev. B **99**, 115121 (2019).

[27] K. Das and A. Agarwal, Linear magnetochiral transport in tilted type-I and type-II Weyl semimetals, Phys. Rev. B **99**, 085405 (2019).

[28] N. Kumar, S. N. Guin, C. Felser, and C. Shekhar, Planar Hall effect in the Weyl semimetal GdPtBi, Phys. Rev. B **98**, 041103(R) (2018).

[29] J. Yang, W. L. Zhen, D. D. Liang, Y. J. Wang, X. Yan, S. R. Weng, J. R. Wang, W. Tong, L. Pi, W. K. Zhu, and C. J. Zhang, Current jetting distorted planar Hall effect in a Weyl semimetal with ultrahigh mobility, Phys. Rev. Materials **3**, 014201 (2019).

[30] K.-S. Kim, Role of axion electrodynamics in a Weyl metal: Violation of Wiedemann-Franz law, Phys. Rev. B **90**, 121108(R) (2014).

[31] R. Lundgren, P. Laurell, and G. A. Fiete, Thermoelectric properties of Weyl and Dirac semimetals, Phys. Rev. B **90**, 165115 (2014).

[32] G. Sharma, P. Goswami, and S. Tewari, Nernst and magnetothermal conductivity in a lattice model of Weyl fermions, Phys. Rev. B **93**, 035116 (2016).

[33] B. Z. Spivak and A. V. Andreev, Magnetotransport phenomena related to the chiral anomaly in Weyl semimetals, Phys. Rev. B **93**, 085107 (2016).

[34] A. Lucas, R. A. Davison, and S. Sachdev, Proc. Natl. Acad. Sci. U.S.A. **113**, 9463 (2016).

[35] Y. Ferreiros, A. A. Zyuzin, J. H. Bardarson, Anomalous Nernst and thermal Hall effects in tilted Weyl semimetals, Phys. Rev. B **96**, 115202 (2017).

[36] S. Saha and S. Tewari, Anomalous Nernst effect in type-II Weyl semimetals, Eur. Phys. J. B **91**, 4 (2018).

[37] Z. Jia, C. Li, X. Li, J. Shi, Z. Liao, D. Yu, and X. Wu, Thermoelectric signature of the chiral anomaly in Cd_3As_2, Nat. Commun. **7**, 13013 (2016).

[38] T. Liang, J. Lin, Q. Gibson, T. Gao, M. Hirschberger, M. Liu, R. J. Cava, and N. P. Ong, Anomalous Nernst Effect in the Dirac Semimetal Cd_3As_2, Phys. Rev. Lett. **118**, 136601 (2017).

[39] J. E. Sipe and A. I. Shkrebtii, Second-order optical response in semiconductors, Phys. Rev. B **61**, 5337 (2000).

[40] E. Deyo, L. E. Golub, E. L. Ivchenko, and B. Spivak, Semiclassical theory of the photogalvanic effect in non-centrosymmetric systems, arXiv:0904.1917v1.

[41] T. Morimoto and N. Nagaosa, Topological nature of nonlinear optical effects in solids, Sci. Adv. **2**, e1501524 (2016).

[42] F. de Juan, A. G. Grushin, T. Morimoto, and J. E. Moore, Quantized circular photogalvanic effect in Weyl semimetals, Nat. Commun. **8**, 15995 (2017).

[43] E. J. König, H.-Y. Xie, D. A. Pesin, and A. Levchenko, Photogalvanic effect in Weyl semimetals, Phys. Rev. B **96**, 075123 (2017).

[44] L. E. Golub and E. L. Ivchenko, Circular and magnetoinduced photocurrents in Weyl semimetals, Phys. Rev. B **98**, 075305 (2018).

[45] X. Yang, K. Burch, and Y. Ran, Divergent bulk photovoltaic effect in Weyl semimetals, arXiv:1712.09363.

[46] Z. Li, Y. Q. Jin, T. Tohyama, T. Iitaka, J. X. Zhang, and H. Su, Second harmonic generation in the Weyl semimetal TaAs from a quantum kinetic equation, Phys. Rev. B **97**, 085201 (2018).

[47] L. Wu, S. Patankar, T. Morimoto, N. L. Nair, E. Thewalt, A. Little, J. G. Analytis, J. E. Moore, and J. Orenstein, Giant anisotropic nonlinear optical response in transition metal monopnictide Weyl semimetals, Nat. Phys. **13**, 350 (2017)

[48] I. Sodemann and L. Fu, Quantum Nonlinear Hall Effect Induced by Berry Curvature Dipole in Time-Reversal Invariant Materials, Phys. Rev. Lett. **115**, 216806 (2015).

[49] Z. Z. Du, C. M. Wang, H.-Z. Lu and X. C. Xie, Band Signatures for Strong Nonlinear Hall Effect in Bilayer WTe_2, Phys. Rev. Lett. **121**, 266601 (2018).

[50] J. I. Facio, D. Efremov, K. Koepernik, J.-S. You, I. Sodemann and J. van den Brink, Strongly Enhanced Berry Dipole at Topological Phase Transitions in BiTeI, Phys. Rev. Lett. **121**, 246403 (2018).

[51] Y. Zhang, Y. Sun and B. Yan, Berry curvature dipole in Weyl semimetal materials: An *ab initio* study, Phys. Rev. B **97**, 041101(R) (2018).

[52] S. S. Tsirkin, P. A. Puente and I. Souza, Gyrotropic effects in trigonal tellurium studied from first principles, Phys. Rev. B **97**, 035158 (2018).

[53] H. Wang and X. Qian, Ferroicity-driven nonlinear photocurrent switching in time-reversal invariant ferroic materials, Sci. Adv. **5**, eaav9743 (2019).

[54] D. F. Shao, S. H. Zhang, G. Gurung, W. Yang and E. Y. Tsymbal, Nonlinear Anomalous Hall Effect for Néel Vector Detection, Phys. Rev. Lett. **124**, 067203 (2020).

[55] O. Matsyshyn and I. Sodemann, Nonlinear Hall Acceleration and the Quantum Rectification Sum Rule, Phys. Rev. Lett. **123**, 246602 (2019).

[56] Y. Gao, F. Zhang, and W. Zhang, Second-order nonlinear Hall effect in Weyl semimetals, Phys. Rev. B **102**, 245116 (2020).

[57] Q. Ma, S.-Y. Xu, H. Shen, D. MacNeill, V. Fatemi, T.-R. Chang, A. M. M. Valdivia, S. Wu, Z. Du, C.-H. Hsu *et al.*, Observation of the nonlinear Hall effect under time-reversal-symmetric conditions, Nature (London) **565**, 337 (2019).

[58] K. Kang, T. Li, E. Sohn, J. Shan, and K. F. Mak, Nonlinear anomalous Hall effect in few-layer WTe_2, Nat. Mater. **18**, 324 (2019).

[59] O. O. Shvetsov, V. D. Esin, A. V. Timonina, N. N. Kolesnikov, and E. V. Deviatov, Nonlinear hall effect in three-dimensional weyl and dirac semimetals, JETP Lett. **109**, 715 (2019).

[60] A. Cortijo, Magnetic-field-induced nonlinear optical responses in inversion symmetric Dirac semimetals, Phys. Rev. B **94**, 235123 (2016).

[61] T. Morimoto, S. Zhong, J. Orenstein, and J. E. Moore, Semiclassical theory of nonlinear magneto-optical responses with applications to topological Dirac/Weyl semimetals, Phys. Rev. B **94**, 245121 (2016).

[62] A. A. Zyuzin and A. Y. Zyuzin, Chiral anomaly and second-harmonic generation in Weyl semimetals, Phys. Rev. B **95**, 085127 (2017).

[63] R. H. Li, O. G. Heinonen, A. A. Burkov, and S. S. L. Zhang, Nonlinear Hall effect in Weyl semimetals induced by chiral anomaly, Phys. Rev. B **103**, 045105 (2021).

[64] Y. Gao, F. Zhang, and W. Zhang, Four-wave mixing of Weyl semimetals in a strong magnetic field, J. Phys.: Condens. Matter **32**, 275502 (2020).

[65] Y. Gao and F. Zhang, Current-induced second harmonic generation of Dirac or Weyl semimetals in a strong magnetic field, Phys. Rev. B **103**, L041301 (2021).

[66] G. Sundaram and Q. Niu, Wave-packet dynamics in slowly perturbed crystals: Gradient corrections and Berry-phase effects, Phys. Rev. B **59**, 14915 (1999).

[67] M. O. Goerbig, J.-N. Fuchs, G. Montambaux, and F. Piéchon, Tilted anisotropic Dirac cones in quinoid-type graphene and α–(BEDT-TTF)$_2$I$_3$, Phys. Rev. B **78**, 045415 (2008).

[68] B. Feng, O. Sugino, R.-Y. Liu, J. Zhang, R. Yukawa, M. Kawamura, T. Iimori, H. Kim, Y. Hasegawa, H. Li, L. Chen, K. Wu, H. Kumigashira, F. Komori, T.-C. Chiang, S. Meng, and I. Matsuda, Dirac Fermions in Borophene, Phys. Rev. Lett. **118**, 096401 (2017).

[69] Y. Wu, H. Liu, H. Jiang, and X. C. Xie, Global phase diagram of disordered type-II Weyl semimetals, Phys. Rev. B **96**, 024201 (2017).

[70] S. P. Mukherjee and J. P. Carbotte, Imaginary part of Hall conductivity in a tilted doped Weyl semimetal with both broken time-reversal and inversion symmetry, Phys. Rev. B **97**, 035144 (2018).

[71] D. T. Son and N. Yamamoto, Kinetic theory with berry curvature from quantum field theories, Phys. Rev. D **87**, 085016 (2013).

[72] D. Xiao, J. Shi, and Q. Niu, Berry Phase Correction to Electron Density of States in Solids, Phys. Rev. Lett. **95**, 137204 (2005).

[73] E. Malic, T. Winzer, E. Bobkin, and A. Knorr, Microscopic theory of absorption and ultrafast many-particle kinetics in graphene, Phys. Rev. B **84**, 205406 (2011).

[74] M. Chang, and M. Yang, Chiral magnetic effect in a two-band lattice model of Weyl semimetal, Phys. Rev. B **91**, 115203 (2015).

[75] C. Xiao, H. Chen, Y. Gao, D. Xiao, A. H. MacDonald, and Q. Niu, Linear magnetoresistance induced by intra-scattering semiclassics of Bloch electrons, Phys. Rev. B **101**, 201410(R) (2020).

[76] J. P. Carbotte, Dirac cone tilt on interband optical background of type-I and type-II Weyl semimetals, Phys. Rev. B **94**, 165111 (2016).

[77] Y. Gao, and B. Ge, Second harmonic generation in Dirac/Weyl semimetals with broken tilt inversion symmetry, Opt. Express **29**, 6903 (2021).

[78] L. Onsager, Reciprocal relations in irreversible processes. I., Phys. Rev. **37**, 405 (1931).

[79] H. B. G. Casimir, On onsager's principle of microscopic reversibility, Rev. Mod. Phys. **17**, 343 (1945).

[80] G. Sharma, P. Goswami, and S. Tewari, Chiral anomaly and longitudinal magnetotransport in type-II Weyl semimetals, Phys. Rev. B **96**, 045112 (2017).

[81] X. Dai, Z. Z. Du, and H. Lu, Negative Magnetoresistance without Chiral Anomaly in Topological Insulators, Phys. Rev. Lett. **119**, 166601 (2017).

[82] A. Cortijo, Linear magnetochiral effect in Weyl semimetals, Phys. Rev. B **94**, 241105(R) (2016).

[83] V. A. Zyuzin, Linear magnetochiral effect in Weyl semimetals, Phys. Rev. B **95**, 245128 (2017).